Relevant Material for Lecture 10

“Galaxies: Structure, Dynamics, and Evolution”

7 Applications to large numbers of galaxies

The simplest diagnostic of a galaxy is its color. Below we show the correlation between color and magnitude for a sample of field galaxies (from SDSS).

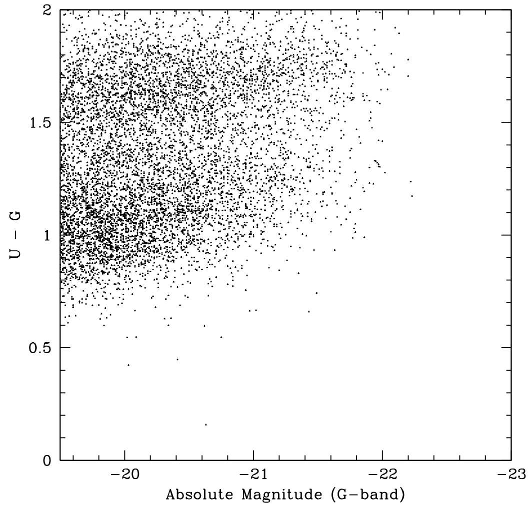

As can be seen, there is a sequence of red galaxies, with U - G colors around 1.7. A typical spectrum is shown below:

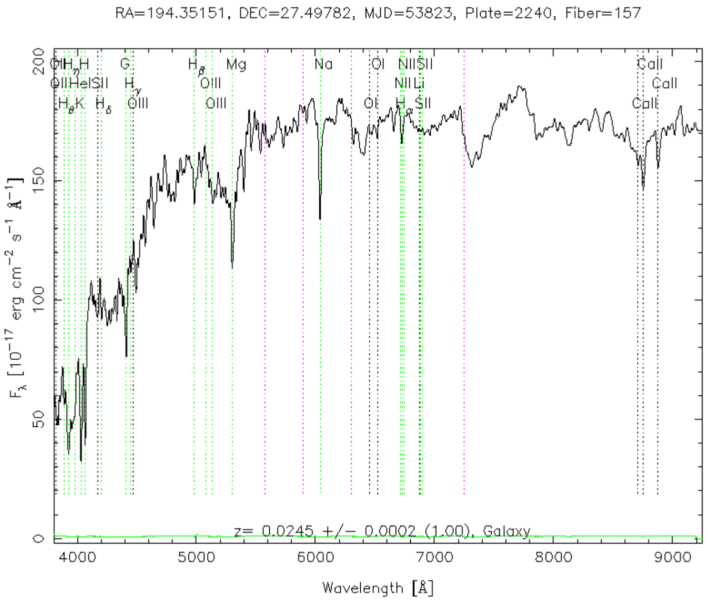

The galaxy has strong absorption lines, including a strong break at 4000 angstrom (rest), strong Mg absorption lines, etc. This is an old galaxy. There is no ongoing star formation.

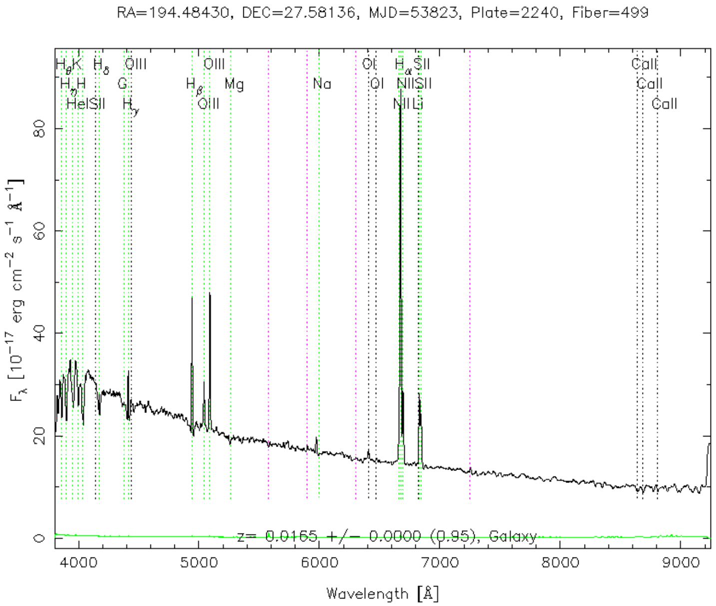

This is a spectrum of a typical blue galaxy. It has strong emission lines, and much weaker absorption lines. It has almost no 4000 Angstrom break, but fairly strong Balmer lines (H gamma, delta, ...) This is a spectrum of a star forming galaxy.

The distinction between the red galaxies and the blue galaxies seems to be mostly one of star forming versus dead galaxies. This is not entirely true - some red galaxies are also star forming, but are red due to dust.

Age determinations

The color of the red sequence galaxies is consistent with an old age (say 10Gyr), and no star formation. This is not unique, however:

- dust can make a blue galaxy look red
- higher metallicity makes a galaxy look redder (at a given age).

Hence, without more information, it is hard to be sure of this age. This is why extensive studies are being made of the detailed absorption lines, leaving metallicity and age a free parameter. Absorption line strengths are less sensitive to dust, so that is less of a concern. These studies generally indicate that the galaxies are indeed old (with variations in age, metallicity, and metal abudance ratios !)

Another constraint can come from the tightness of the red sequence. In clusters, the red sequence is very tight.

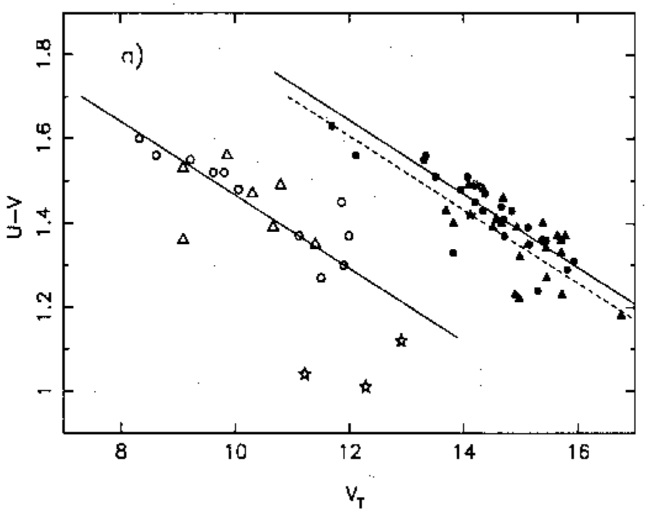

Color magnitude of the Virgo and Coma cluster (Bower et al 1992). The small spread in colors indicate a small spread in age.

The measured scatter in U-V color is 0.05 mag, of which 0.03 is due to observational error.

In the previous handout, we saw that colors evolve with time as $color = a\ log(t) + b$. For the U-V color, the coefficient a is about 0.65. Hence a scatter of 0.05 mag in U-V indicates a scatter of 0.08 in log(age), which is very low - a typical factor of 1.2, or 20%. Hence the red galaxies are very uniform, with small scatter in age.

Systematic analysis of the SDSS galaxies

Kauffmann et al (2003a,b, 2004), Brinchmann et al (2004) analyzed the spectra of $> 1e5$ galaxies from SDSS. They determined stellar masses and star formation rates. They used absorption and emission lines - not just colors

The great advantage of using absorption lines is that they are less influenced by dust than colors. But the effects of dust are not zero - young stars are preferentially more obscured than old stars. Hence the absorption line strengths (which are expressed in equivalent width) can still be influenced by dust if some populations are more extincted than others. This is ignored in the models used below.

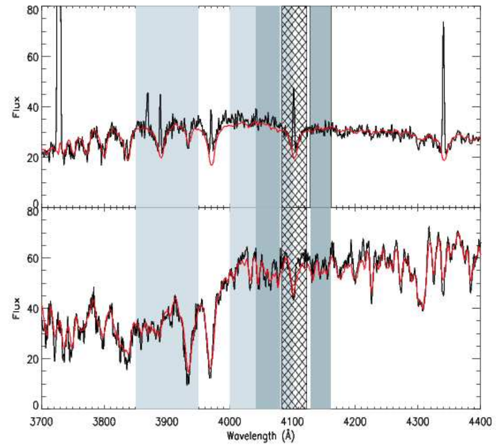

Figure 1. SDSS spectra of a late-type galaxy (top) and an early-type galaxy (bottom) are plotted over the interval 3700–4400 Å in the restframe. The red line shows our best-fitting BC2003 model spectrum. The light grey-shaded regions indicate the bandpasses over which the $D_n(4000)$ index is measured. The dark grey regions show the pseudocontinua for the $H\delta_A$ index, while the hatched region shows the $H\delta_A$ bandpass.

This figure shows the main indices used in the study for the stellar mass determination, the 4000 Å break and Hδ.

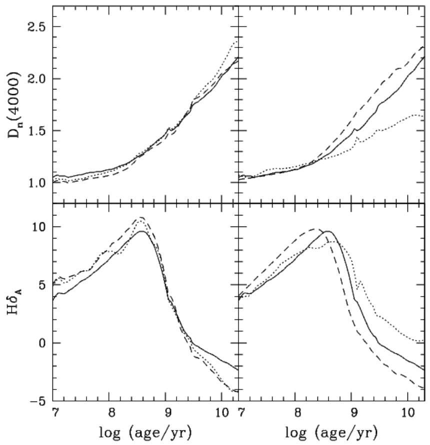

Figure 2. Left: the evolution of $D_n(4000)$ and $H\delta_A$ following an instantaneous, solar-metallicity burst of star formation. Solid lines show results from BC2003+STELIB, the dotted line shows results if the Pickles (1998) library is used, and the dashed line is for the Jacoby et al. (1984) library. Right: the evolution of $D_n(4000)$ and $H\delta_A$ for bursts of different metallicity. The solid line is a solar metallicity model, the dotted line is a 20 per cent solar model and the dashed line as a 2.5 solar model.

These parameters depend on age as shown above. Notice that D4000 increases steadily with age, whereas Hδ peaks around 300 Myrs. Hence it is sensitive to star formation in the last Gyr.

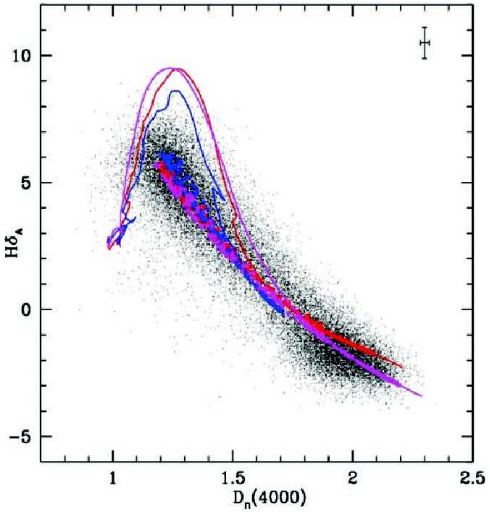

Figure 3. $H\delta_A$ is plotted as a function of $D_n(4000)$ for 20 per cent solar, solar and 2.5 times solar metallicity bursts (blue, red and magenta lines), and for 20 per cent solar, solar and 2.5 solar continuous star formation histories (blue, red and magenta symbols). A subset of the SDSS data points with small errors are plotted as black dots. The typical error bar on the observed indices is shown in the top right-hand corner of the plot.

When we measure the parameters for galaxies, the two correlate as shown in the figure above. For ordinary models with continuous star formation, H δ goes down, and D4000 increases, and a good correlation exists. However bursts super imposed on continuous star formation give H δ which deviates.

The combination of Hδ and D4000 gives a good constraint on the stellar population of the galaxy, and its mass-to-light ratio. However, the extinction also needs to be measured. The colors are used for that. Here is the result:

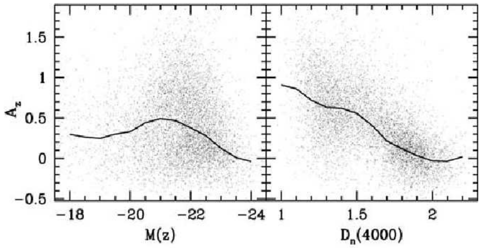

Figure 12. Left: A_z is plotted as a function of z-band absolute magnitude for a random subsample of galaxies. The solid line shows the running median of the distribution for the full sample. Right: A_z is plotted as a function of $D_n(4000)$.

The galaxies with high D4000 have low extinction estimated, star forming galaxies have much higher extinction (as might be expected). Now the mass-to-light ratio can be estimated, from D4000, Hδ and A_z. Below the derived mass-to-light ratio is plotted against color.

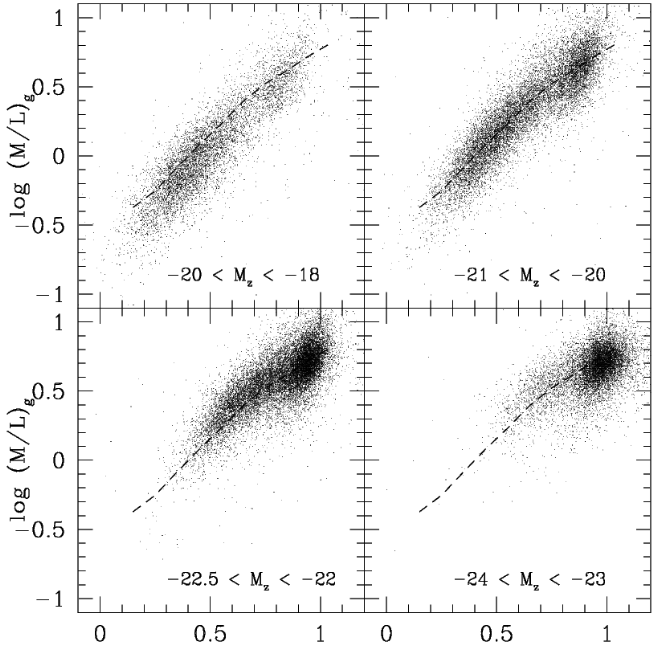

Figure 20. The g-band mass-to-light ratio is plotted as a function of the $g - r$ colour (K-corrected to $z = 0.1$) for galaxies in four different bins of z-band absolute magnitude. The dashed line shows the mean relation evaluated for galaxies with $-21 < M(z) < -20$.

There is clearly a good relation between the derived mass-to-light ratio and the color. Furthermore, the stellar masses correlate well with the dynamical masses (not shown in the paper, plotted myself)

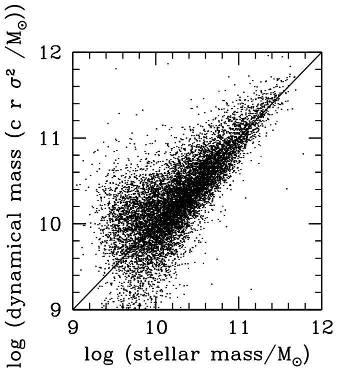

Hence the stellar masses we have now are reliable.

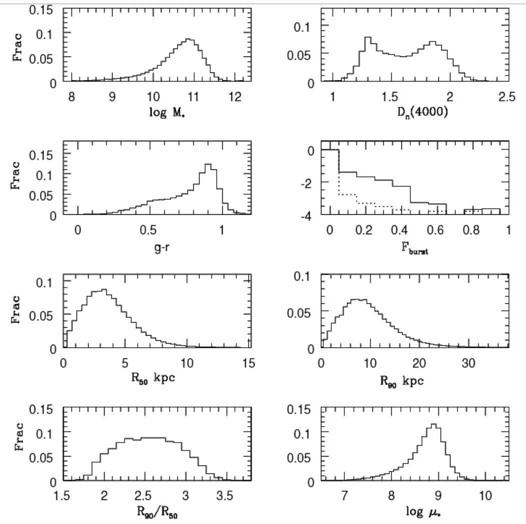

Figure 21. The fraction of the total stellar mass in the Universe contained in galaxies as a function of (i) log stellar mass, (ii) D$_n$(4000), (iii) $g-r$ colour (K-corrected to $z = 0.1$, (iv) $F_{\rm burst}$(median) solid and $F_{\rm burst}$ (2.5 per cent) dotted, (v) Petrosian half-light radius in the r band, (vi) Petrosian 90 per cent radius on the r band, (vii) concentration index (R_{90}/R_{50}), (viii) log surface mass density. The fraction is shown linearly in all plots except that for $F_{\rm burst}$ where the logarithm is given.

We can now analyze the distribution of galaxies over mass, color, etc. This is shown above.

Our main conclusions are as follows.

(i) The characteristic mass $M_{\rm char}$ of galaxies at the present day, defined as the peak of the distribution function shown in the top left-hand panel of Fig. 21, is 6×10^{10} $\mathrm{M}_\odot$. This agrees reasonably well with the results of Cole et al. (2001). These authors transform the near-infrared luminosity function derived from 2dF/2MASS data to a stellar mass function using a colour-based technique. Their Schechter-function parametrization yields $M_{\rm char} = 5.6 \times 10^{10}$ $\mathrm{M}_\odot$ for $H_0 = 70$ km s^{-1} Mpc^{-1} and a Kennicutt (1983) IMF, which is fairly close to the Kroupa (2001) IMF that we have assumed.

We find that only 20 per cent of the total stellar mass is contained in galaxies less massive than 10^{10} $\mathrm{M}_\odot$. An even smaller fraction ($\sim$13 per cent) of the total mass is contained in galaxies less massive than 10^9 $\mathrm{M}_\odot$. The total stellar mass budget of the Universe is thus heavily weighted towards galaxies that are within a factor of 10 in mass of the Milky Way.

(ii) The $\mathrm{D}_n(4000)$ distribution of the stellar mass is strongly bimodal. The first peak is centred at $\mathrm{D}_n(4000) \sim 1.3$. Galaxies with break strengths of this value have r-band weighted mean stellar ages of $\sim$1–3 Gyr and mass-weighted mean ages a factor of $\sim$2 larger. Almost all of these galaxies also have emission lines and are thus forming stars at the present day. The second peak is centred at $\mathrm{D}_n(4000) \sim 1.85$, a value typical of old elliptical galaxies with mean stellar ages $\sim$10 Gyr.

(iii) The $g - r$ colour distribution exhibits a strong red peak, but the blue peak is much less pronounced. This is probably because colours depend both on stellar age and on dust attenuation, whereas $\mathrm{D}_n(4000)$ is not affected by dust. Note that Strateva et al. (2001) have also discussed the bimodality in the colour distributions of SDSS galaxies.

(iv) The vast majority ($>$90 per cent) of the stellar mass is in galaxies that have not formed more than 5 per cent of the stars in a burst over the past 2 Gyr.

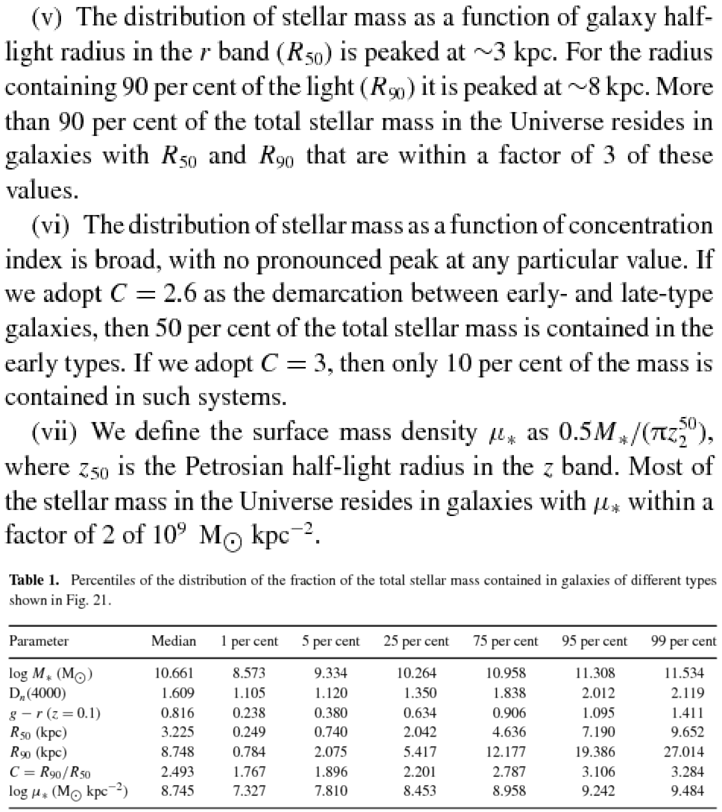

(v) The distribution of stellar mass as a function of galaxy half-light radius in the r band (R_{50}) is peaked at ~3 kpc. For the radius containing 90 per cent of the light (R_{90}) it is peaked at ~8 kpc. More than 90 per cent of the total stellar mass in the Universe resides in galaxies with R_{50} and R_{90} that are within a factor of 3 of these values.

(vi) The distribution of stellar mass as a function of concentration index is broad, with no pronounced peak at any particular value. If we adopt $C = 2.6$ as the demarcation between early- and late-type galaxies, then 50 per cent of the total stellar mass is contained in the early types. If we adopt $C = 3$, then only 10 per cent of the mass is contained in such systems.

(vii) We define the surface mass density μ_* as $0.5M_*/(\pi z_2^{50})$, where z_{50} is the Petrosian half-light radius in the z band. Most of the stellar mass in the Universe resides in galaxies with μ_* within a factor of 2 of 10^9 $M_\odot$ kpc^{-2}.

Table 1. Percentiles of the distribution of the fraction of the total stellar mass contained in galaxies of different types shown in Fig. 21.

Parameter	Median	1 per cent	5 per cent	25 per cent	75 per cent	95 per cent	99 per cent
log M_* ($M_\odot$)	10.661	8.573	9.334	10.264	10.958	11.308	11.534
$D_n(4000)$	1.609	1.105	1.120	1.350	1.838	2.012	2.119
$g - r$ ($z = 0.1$)	0.816	0.238	0.380	0.634	0.906	1.095	1.411
R_{50} (kpc)	3.225	0.249	0.740	2.042	4.636	7.190	9.652
R_{90} (kpc)	8.748	0.784	2.075	5.417	12.177	19.386	27.014
$C = R_{90}/R_{50}$	2.493	1.767	1.896	2.201	2.787	3.106	3.284
log μ_* ($M_\odot$ kpc^{-2})	8.745	7.327	7.810	8.453	8.958	9.242	9.484

The next aspect to study is to analyze how galaxy properties depend on mass, and other parameters. First we analyze the mass dependence (Kauffmann et al 2003b).

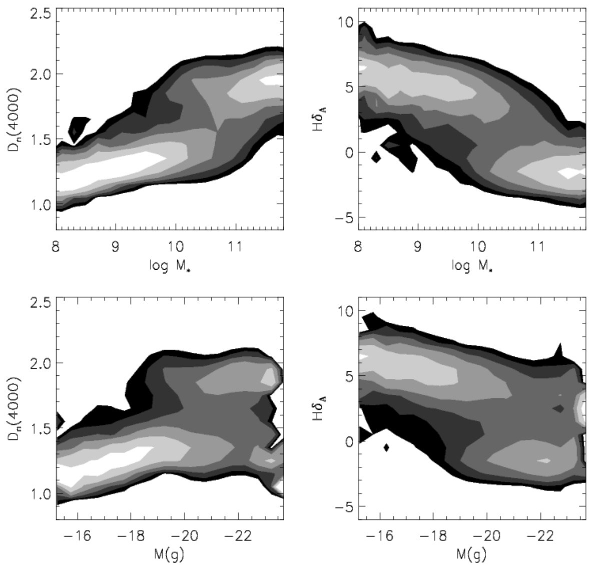

Figure 1. Conditional density distributions showing trends in the stellar age indicators $D_n(4000)$ and $H\delta_A$ as functions of the logarithm of stellar mass and of g-band absolute magnitude. Galaxies have been weighted by $1/V_{\max}$ and the bivariate distribution function has been normalized to a fixed number of galaxies in each bin of log M_* or $M(g)$. Here and in all subsequent contour plots, each contour represents a factor of 2 change in density.

Galaxies below 2e10 Msun are quite different from galaxies above 2e10 Msun !

Below 2e10: mostly low D4000 $->$ young, forming stars

Above 2e10: mostly high D4000 $->$ old , not forming stars in large numbers

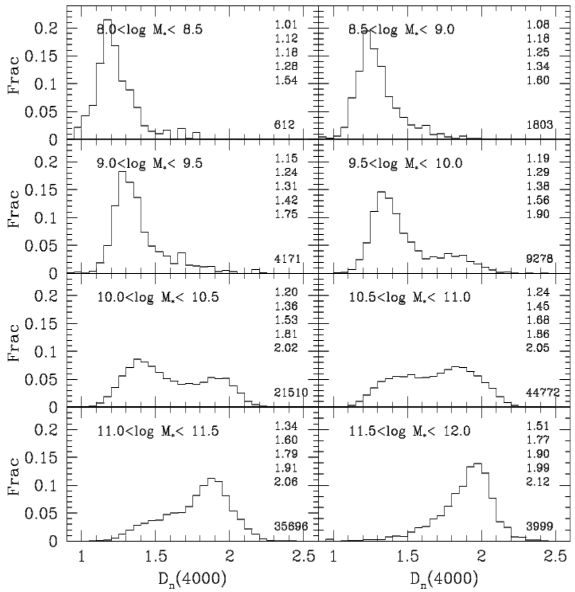

Figure 2. Histograms showing the fraction of galaxies as a function of $D_n(4000)$ in eight different ranges of stellar mass. The numbers in the upper right-hand corner of each panel list, from top to bottom, the fifth, 25th, 50th, 75th and 95th percentiles of the distribution. The number in the lower right-hand corner is the number of galaxies contributing to the histogram.

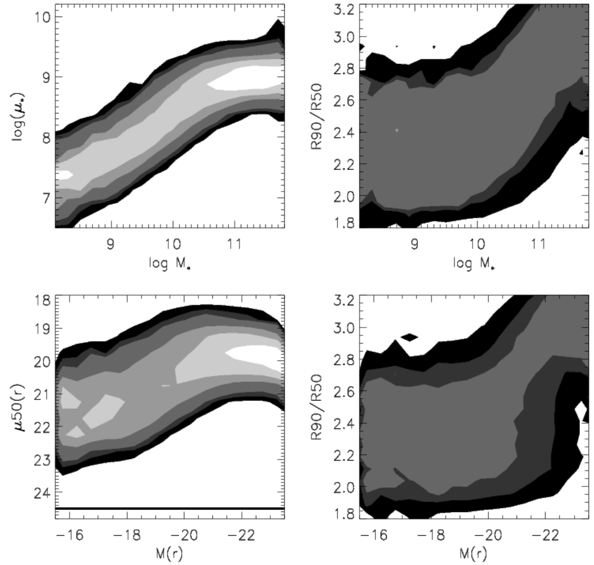

Figure 8. Conditional density distributions showing trends in the structural parameters μ_*, $\mu_{1/2}$ and $C = R90/R50$ as a function the logarithm of stellar mass and as a function of r-band absolute magnitude. Galaxies have been weighted by $1/V_{\rm max}$ and the bivariate distribution function has been normalized to a fixed number of galaxies in each bin of log M_* and of r-band absolute magnitude. The line in the bottom left-hand panel indicates the surface brightness completeness limit of the SDSS survey.

Surface density, and concentration, also depend on M. Surface density is $Mstar/R^2$. Concentration is R(90)/R(50): the ratio of the radii which encompass 90% and 50% of the light, respectively. High concentration means high sersic index, low concentration means low sersic index. hence galaxies with mass $>$ 1e11 all have high sersic index, galaxies with masses $<$ 2e10 all have low sersic index (are exponential disks)

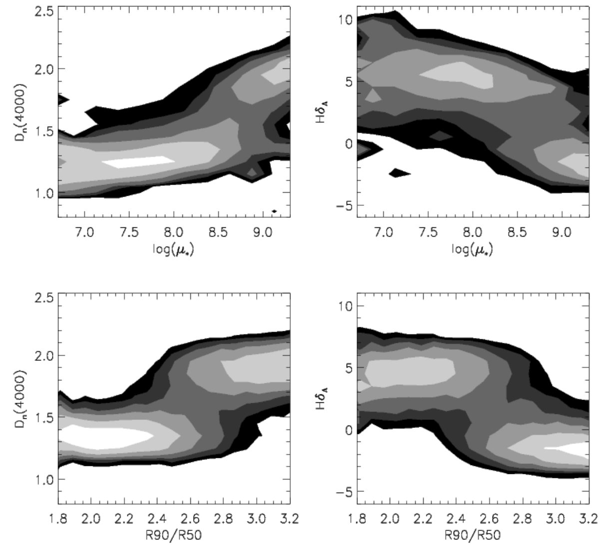

Figure 12. Conditional density distributions showing trends in the stellar age indicators D$_n$(4000) and Hδ_A as functions of the logarithm of the surface mass density μ_* and of the concentration index C.

Finally, D4000 correlates better with stellar surface density than with mass. The plot above shows a tight relation between D4000 with density - little overlap where both high and low values occur.

Star formation rates

Next we determine the star formation rate. This was done primarily from the emission lines, H α and other lines. See Brinchman et al 2004 for details. Corrections for extinction, and aperture effects were very important.

The specific star formation rate $SFR/Mstar$ is shown against mass

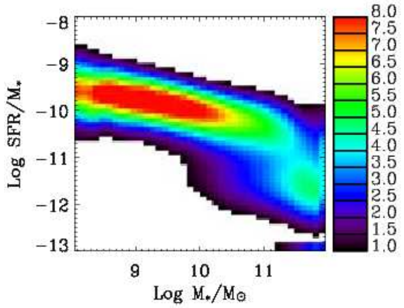

Clearly, the low mass galaxies have *relatively* more star formation than the high mass galaxies, i.e., they formed relatively speaking more of their stars in recent times.

Environment

As we saw earlier, rich clusters consist mostly of red galaxies - not blue. They are quite different from the normal field.

In order to measure this properly, we have to define the “environment” of a galaxy - indicating whether it lies in a cluster or not. We do that by counting the galaxies around the galaxy. If that number is high, it is a “high density”, if it is low, it is “low density”.

We either use this “density” parameter, or the number of neighbors, as shown below (Kauffmann et al. 2004):

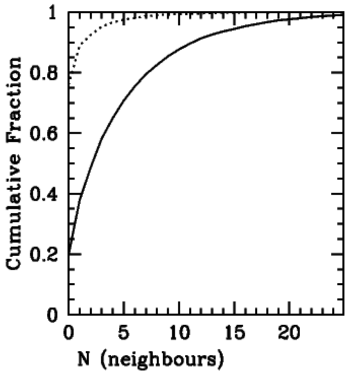

Figure 1. The cumulative fraction of galaxies with counts less than N for the target sample (solid curve) and for a random sample (dotted curve).

Only a small fraction of galaxies are in really rich clusters (> 20 neighbors)

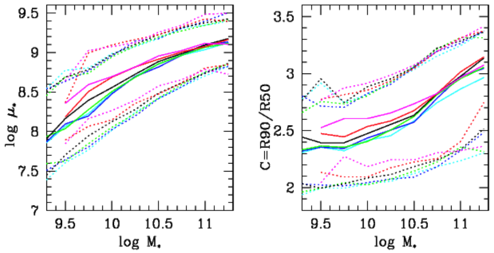

Figure 5. The relations between surface mass density and stellar mass (left) and concentration index and stellar mass (right) are plotted for galaxies in six different density bins as follows: cyan, 0 or 1 neighbour; blue, 2–3 neighbours; green, 4–6 neighbours; black, 7–11 neighbours; red, 12–16 neighbours; magenta, 17 or more neighbours. The solid curves indicate the median value of log μ_* or C and a given value of log M_*. The dotted lines indicate the 10th and 90th percentiles of the distributions.

This shows how the stellar density, and the concentration depends on mass. The black line shows the dependence for the full sample, the colored lines for high and low density. There is not much difference !

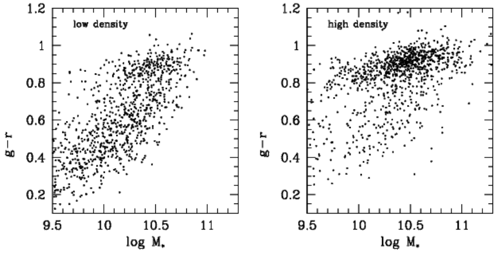

Figure 6. A scatterplot of $g - r$ colour versus stellar mass is plotted for 1000 galaxies in our lowest-density bin ($N_{\rm neighb} = 0$–1; left) and our highest-density bin ($N_{\rm neighb} > 17$; right).

The colors are very different, however ! Here we see the g-r color mass diagram, for low density and high density environments. Look at how different ! There are many more red galaxies in high density environments, at a given mass. You can also see that there are more high mass galaxies in dense environments.

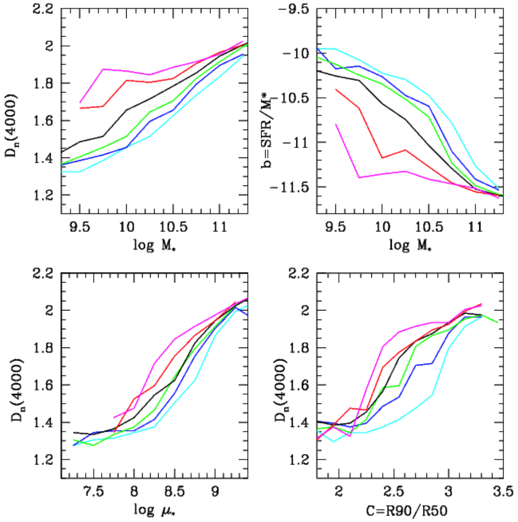

Figure 7. Top: the median relations between $D_n(4000)$ and SFR/M_* are plotted as a function of stellar mass for five different bins in density, colour-coded as in Fig. 5. Bottom: the median relations between $D_n(4000)$ and μ_* (left) and C (right).

The same thing holds for D4000 and star formation rate (estimated from the emission lines). The star formation rate is characterised by the specific star formation rate $SFR/Mstar$. This parameter is independent of mass - it is inversely proportional to the time it takes to build the galaxy at its current star formation rate. Hence old galaxies have low b, and young galaxies high b.
Blue lines show the relation for low density environments (low D4000, high b). Red lines for high density environments (high D4000, low b)
Density has a distinct impact on the star formation history ! But not very much on the size, or concentration.

This last result came as a surprise: classical studies had always shown that clusters have many more ellipticals and S0's than the field. The field is more dominated by spirals. Spirals are very different from ellipticals and S0's: they form stars, and have large disks. Hence the SDSS results confirm that the field has more star forming galaxies, but does not confirm that the galaxies are larger in the field.
How come ?
This is due to the fact that we study galaxy parameters as a function of stellar mass.
The rich environments have more massive galaxies than the field; but at each mass, the galaxies are similar, except for the star formation rate. The previous samples were not studied by mass, but by luminosity - and hence the results looked different.

Main result
1) High mass galaxies have nearly formed all their stars
2) Galaxies in rich environments have less star formation
These two results suggest that stellar mass *and environment* determine the star formation history. The environment is correlated to the type of halo the galaxy sits in. So maybe it is just 1 parameter which determines the star formation history: the halo mass.
In more massive halos, galaxies have lower star formation. It could be that the correlation with galaxy mass is entirely due to the halo - more massive galaxies are likely to sit in more massive halos.
The physics behind this are under active research right now!